JOURNAL OF GUIDANCE, CONTROL, AND DYNAMICS
Vol. 22, No. 4, July–August 1999

Optimal Combined Reaction-Wheel Momentum Management for Earth-Pointing Satellites

Xiaojiang Chen,* Willem H. Steyn,† Stephen Hodgart,‡ and Yoshi Hashida§
University of Surrey, Guildford, England GU2 5XH, United Kingdom

When reaction wheels of a satellite drift toward saturation caused by the accumulated effect of external torque, it is common to employ thrusters or magnetorquers to actively unload extra momentum of the wheels. This paper presents several optimal approaches to manage the three-axis reaction wheel momentum of Earth-pointing satellites actuated by three-axis magnetorquers and/or thrusters. The optimal momentum dumping using magnetorquers only behaves fairly slowly, and there are difficulties in solving a two-point boundary problem for onboard applications. Comparatively, thrusters can achieve relatively fast momentum dumping at the cost of consuming expendable fuel. Based upon relatively simple optimal algorithms using thrusters only, the newly proposed combined algorithms effectively separate the required torques for magnetorquers and thrusters commanding simultaneously. They simply employ on-line geomagnetic measurements. The key benefit of these combined approaches is that they can save a large amount of thruster propellant because of the assistance of the magnetorquers. The realistic simulations showed that the optimal combined method can economize at least 20% thruster fuel within an unloading time of $\frac{1}{10}$ of an orbit (about 10 min) for a low-Earth-orbit mini-satellite. The combined controllers are readily applicable to real-time practical momentum dumping.

I. Introduction

EARTH-POINTING satellites are expected to maintain the local-vertical/local-horizontal attitude in the presence of environmental disturbance effects. Generally, this requires a spacecraft reaction-wheel (RW) system to exchange momentum continuously with the spacecraft body. The secular external disturbance torques, for example, the torques caused by passive gravity gradient, aerodynamic and solar forces, and active control torques from thrusters and magnetorquers, will tend to make the wheels drift toward saturation. Therefore, management of three-axis reaction wheel momentum is required to counteract the influence of persistent external disturbance torques. Usually an external torque must be applied, employing thrusters or magnetorquers, to force the wheel speed back to nearly zero momentum.

A number of relevant studies have been presented to cope with momentum dumping techniques. Johnson and Skelton[1] proposed an optimal desaturation control scheme by using the natural environmental torques (gravity gradient, aerodynamic, etc.). Their solution of the optimization problem is a time-varying feedback gain matrix for the system state to obtain an angular rate reference command vector for the spacecraft. In Ref. 2 a periodic disturbance accommodating control law was investigated for asymptotic momentum management of control moment gyros of the space station. A new sequential design procedure for an optimal control moment gyro momentum management and attitude control system was discussed by Sunkel and Shieh.[3] An inexpensive but slow unloading of RW momentum can be carried out by employing magnetorquers.[4–9] Iida and Keiken[4] addressed a new magnetic angular momentum management method that incorporates environmental disturbance torque estimation and an unloading controller over an orbital period. Glaese et al.[5] described a minimum energy desaturation law to dump angular momentum on an inertially stabilized space telescope. They also considered the simpler but more inefficient cross-product law. Burns and Flashner[6] presented an adaptive control technique making use of simultaneous magnetic, gravity gradient, and aerodynamic torques for momentum unloading of three-axis stabilized, nadir-pointing spacecraft. Chang[7] used magnetorque to contain the momentum bias on a single wheel, three-axis inertially stabilized satellite at a nominal value. He proposed a simple penalty factor law to reduce the undesirable disturbance torques during magnetotorquing. A comparison of optimal desaturation algorithms with the conventional cross-product law (CCPL), using three-axis magnetorquers for a nadir-pointing, three-axis RW stabilized satellite in a circular orbit, was analyzed in detail by Steyn.[8]

The effective and rapid momentum dumping can be achieved by thrusters at the cost of expendable propellant consumption.[10,11] For satellites with thrusters, the minimization of thruster propellant dissipation is critically important to the space mission. To implement propellant saving as well as rapid momentum dumping, we will discuss several novel combined control methods, simultaneously using three-axis magnetorquers and thrusters to obtain a tradeoff between the dumping rate and propellant usage.

The paper is organized as follows. In Sec. II we derive the general model of Earth-pointing RW momentum dumping. Then in Secs. III and IV the optimal linear quadratic regulator (LQR) and minimum energy controllers (MEC) using magnetorquers and pulse-width modulated (PWM) thrusters are described separately. Subsequently, in Sec. V the optimal combined control schemes are analyzed. In Secs. VI and VII the comparison of the control performance for different algorithms is shown.

II. Wheel Momentum Management Model of Rigid Satellites

The dynamic model of an Earth-pointing satellite using three-axis reaction wheels as internal torque actuators and magnetorquers and thrusters as external torque actuators, and ignoring the small change of spacecraft inertia tensor caused by thruster propellant consumption, is given by

$$\boldsymbol{I}\dot{\boldsymbol{\omega}}_{\mathrm{BY}} = \boldsymbol{N}_T + \boldsymbol{N}_M + \boldsymbol{N}_{\mathrm{GG}} + \boldsymbol{N}_D - \boldsymbol{\omega}_{\mathrm{BY}} \times (\boldsymbol{I}\boldsymbol{\omega}_{\mathrm{BY}} + \boldsymbol{h}) - \dot{\boldsymbol{h}} \quad (1)$$

where $\boldsymbol{\omega}_{\mathrm{BY}}$, $\boldsymbol{I}$, $\boldsymbol{h}$, $\boldsymbol{N}_M$, $\boldsymbol{N}_T$, and $\boldsymbol{N}_{\mathrm{GG}}$ are, respectively, the inertially referenced body angular velocity vector, moment of inertia of spacecraft, three-axis RW angular momentum vector, applied torque vector by three-axis magnetorquers, applied torque vector by three-axis thrusters, external disturbance torque vector including the torques caused by the aerodynamic and solar forces, and gravity gradient torque vector. We assume the satellite is three-axis stabilized in a

Received 15 April 1998; revision received 15 January 1999; accepted for publication 28 January 1999.

*Ph.D. Student, Spacecraft Attitude Determination and Control System, Department of Electronic and Electrical Engineering, Surrey Space Center.
†Team Leader of Spacecraft Attitude Determination and Control System, Surrey Space Center.
‡Lecturer, Spacecraft Attitude Determination and Control System, Department of Electronic and Electrical Engineering, Surrey Space Center.
§Research Staff, Spacecraft Attitude Determination and Control System, Surrey Space Center.

circular orbit, and then

$$\boldsymbol{\omega}_{\mathrm{BY}} = \boldsymbol{\omega}_{\mathrm{LO}} + \boldsymbol{T}_{\mathrm{BYLO}}\boldsymbol{\omega}_0, \qquad \boldsymbol{T}_{\mathrm{BYLO}} = \begin{bmatrix} A_{11} & A_{12} & A_{13} \\ A_{21} & A_{22} & A_{23} \\ A_{31} & A_{32} & A_{33} \end{bmatrix} \tag{2}$$

$$\boldsymbol{\omega}_0 = [0 \quad -\omega_0 \quad 0]^T$$

where $\boldsymbol{\omega}_{\mathrm{LO}}$ is the relative body angular rate with respect to the local orbital coordinates, $\boldsymbol{T}_{\mathrm{BYLO}}$ is the attitude matrix from local orbital to body coordinates, and $\boldsymbol{\omega}_0$ is a constant orbital angular rate vector. If we assume a fixed Earth-pointing attitude with nadir or off-nadir pointing during RW momentum dumping process, we have

$$\boldsymbol{\omega}_B^O = [\omega_{ox} \quad \omega_{oy} \quad \omega_{oz}]^T = [0 \quad 0 \quad 0]^T$$

and we can also assume a constant attitude matrix $\boldsymbol{T}_{\mathrm{BYLO}}$ and a constant torque vector $\boldsymbol{N}_{\mathrm{GG}}$.[8,10] Furthermore, we define

$$\boldsymbol{N}_{\mathrm{con}} = -\boldsymbol{\omega}_{\mathrm{BY}} \times \boldsymbol{I}\boldsymbol{\omega}_{\mathrm{BY}} + \boldsymbol{N}_{\mathrm{GG}} \tag{3}$$

According to Eq. (2), this torque will also be a constant under the assumption of a fixed Earth-pointing attitude.

The magnetic torque vector $\boldsymbol{N}_M$ in Eq. (1) can be written as the cross product of the magnetic dipole moment $\boldsymbol{M}$ of the three-axis magnetic coils with the measured magnetic field strength $\boldsymbol{B}$ (typically obtained with a three-axis magnetometer):

$$\boldsymbol{N}_M = \boldsymbol{M} \times \boldsymbol{B} = \boldsymbol{Q}(t)\boldsymbol{M} \tag{4}$$

where $\boldsymbol{M}$ is magnetic dipole control moment vector and

$$\boldsymbol{Q}(t) = \begin{bmatrix} 0 & B_z(t) & -B_y(t) \\ -B_z(t) & 0 & B_x(t) \\ B_y(t) & -B_x(t) & 0 \end{bmatrix} \tag{5}$$

The measured magnetic field $\boldsymbol{B}$ along the body frame can be given by

$$\boldsymbol{B} = \boldsymbol{T}_{\mathrm{BYLO}}\boldsymbol{B}_o \tag{6}$$

where $\boldsymbol{B}_o$ is the geomagnetic field vector in the local orbital coordinates. Therefore, the RW momentum desaturation model with a fixed Earth-pointing attitude in a circular orbit can be represented as (ignoring the weak effect of the small external disturbance torque $\boldsymbol{N}_D$)

$$\dot{\boldsymbol{h}}(t) = \boldsymbol{W}\boldsymbol{h}(t) + [\boldsymbol{N}_T + \boldsymbol{Q}(t)\boldsymbol{M} + \boldsymbol{N}_{\mathrm{con}}] \tag{7}$$

with

$$\boldsymbol{W} = \begin{bmatrix} 0 & -\omega_o A_{32} & \omega_o A_{22} \\ \omega_o A_{32} & 0 & -\omega_o A_{12} \\ -\omega_o A_{22} & \omega_o A_{12} & 0 \end{bmatrix} = \text{constant matrix}$$

Accordingly, Eq. (7) can be regarded as the general model for the management of three-axis RW momentum on Earth-pointing satellites. This model implies that only if the torques generated by a three-axis reaction wheel are equal to the sum of the satellite gyroscopic torques, active torque by three-axis magnetorquers, cold-gas thrusters and external disturbances, the satellite will keep the fixed required Earth-pointing attitude, and the RW momentum can be managed by external torques to the expected values.

For the perfect nadir-pointing case ($\boldsymbol{N}_{\mathrm{con}} = 0$) the RW momentum dumping model could be simplified by Steyn[8]:

$$\dot{\boldsymbol{h}}(t) = \boldsymbol{W}\boldsymbol{h}(t) + [\boldsymbol{N}_T + \boldsymbol{Q}(t)\boldsymbol{M}] \tag{8}$$

where

$$\boldsymbol{W} = \begin{bmatrix} 0 & 0 & \omega_o \\ 0 & 0 & 0 \\ -\omega_o & 0 & 0 \end{bmatrix} \tag{9}$$

III. Optimal Desaturation Controllers Using Magnetorquers

A. Linear Quadratic Controllers

Steyn[8] in his thesis has developed several optimal desaturation algorithms using three-axis magnetorquers for the perfect nadir-pointing case in Eq. (8). Here, an optimal feedback control law to regulate the wheel momentum vector $\boldsymbol{h}$ toward the zero vector for the general model in Eq. (7) is to be derived by minimizing the following cost function:

$$J = \frac{1}{2}\int_{t_0}^{t_f} \{\boldsymbol{h}^T\boldsymbol{F}\boldsymbol{h} + \boldsymbol{M}^T\boldsymbol{R}\boldsymbol{M}\}\,\mathrm{d}t \tag{10}$$

where t_0 and t_f are the initial and final time, $\boldsymbol{F}$ is a non-negative symmetric weighting 3×3 matrix for the wheel angular momentum, and $\boldsymbol{R}$ is a positive symmetric weighting 3×3 matrix for the magnetic coil moments. To minimize the cost function in Eq. (10), subject to the desaturation model constraint of Eq. (7) without the term of $\boldsymbol{N}_T$, we get the Hamiltonian function

$$H = \tfrac{1}{2}\boldsymbol{h}^T\boldsymbol{F}\boldsymbol{h} + \boldsymbol{M}^T\boldsymbol{R}\boldsymbol{M} + \boldsymbol{p}^T(t)[\boldsymbol{W}\boldsymbol{h} + \boldsymbol{Q}(t)\boldsymbol{M} + \boldsymbol{N}_{\mathrm{con}}] \tag{11}$$

where $\boldsymbol{p}(t)$ is a costate vector. According to the Pontryagin's principle of optimal theory,[12] we can get the control equation

$$\boldsymbol{M}(t) = -\boldsymbol{R}^{-1}\boldsymbol{Q}^T(t)\boldsymbol{p}(t) \tag{12}$$

and the adjoint equation

$$\dot{\boldsymbol{p}}(t) = -\frac{\partial H}{\partial \boldsymbol{h}} = -\boldsymbol{F}\boldsymbol{h} - \boldsymbol{W}^T\boldsymbol{p}(t) \tag{13}$$

We define the costate to be

$$\boldsymbol{p}(t) = \boldsymbol{K}(t)\boldsymbol{h} - \boldsymbol{g}(t) \tag{14}$$

where $\boldsymbol{K}(t)$ is a time-dependent 3×3 gain matrix and $\boldsymbol{g}(t)$ is a time-dependent 3×1 vector. Using the relation of Eqs. (7) and (12–14), we can then get

$$[\dot{\boldsymbol{K}}(t) + \boldsymbol{K}(t)\boldsymbol{W} + \boldsymbol{F} + \boldsymbol{W}^T\boldsymbol{K}(t) - \boldsymbol{K}(t)\boldsymbol{Q}(t)\boldsymbol{R}^{-1}\boldsymbol{Q}^T(t)\boldsymbol{K}(t)]\boldsymbol{h} + \left[\boldsymbol{K}(t)\boldsymbol{Q}(t)\boldsymbol{R}^{-1}\boldsymbol{Q}^T(t)\boldsymbol{g}(t) + \boldsymbol{K}(t)\boldsymbol{N}_{\mathrm{con}} - \dot{\boldsymbol{g}}(t) - \boldsymbol{W}^T\boldsymbol{g}(t)\right] = 0 \tag{15}$$

If Eq. (15) is always true for any value of $\boldsymbol{h}$, we can obtain a matrix Riccatti equation

$$\dot{\boldsymbol{K}}(t) = -\boldsymbol{K}(t)\boldsymbol{W} - \boldsymbol{W}^T\boldsymbol{K}(t) - \boldsymbol{F} + \boldsymbol{K}(t)\boldsymbol{Q}(t)\boldsymbol{R}^{-1}\boldsymbol{Q}^T(t)\boldsymbol{K}(t) \tag{16}$$

and the differential equation

$$\dot{\boldsymbol{g}}(t) = -[\boldsymbol{W}^T - \boldsymbol{K}(t)\boldsymbol{Q}(t)\boldsymbol{R}^{-1}\boldsymbol{Q}^T(t)]\,\boldsymbol{g}(t) + \boldsymbol{K}(t)\boldsymbol{N}_{\mathrm{con}} \tag{17}$$

The matrix differential Eqs. (16) and (17) must be solved by backward integration according to the two-point boundary value.[8] First, the unknown $\boldsymbol{K}(t_f)$ is chosen as the zero matrix, and Eq. (16) is integrated backward until $\boldsymbol{K}(t_0)$ is found. Then $\boldsymbol{K}(t_f)$ is taken as the $\boldsymbol{K}(t_0)$ of the first iteration, and the integration process is repeated to find the orbital solution for $\boldsymbol{K}(t)$. Finally, substitute the solution $\boldsymbol{K}(t)$ into Eq. (17) to solve $\boldsymbol{g}(t)$. The values of $\boldsymbol{K}(t)$ and $\boldsymbol{g}(t)$ at sampled intervals can then be stored in an onboard look-up table to be used at the corresponding orbital locations for desaturation control.

As an alternative, a fairly accurate quasistatic LQR feedback control law can be computed by an on-line solution of the infinite-time LQR (ILQR) control problem at every sample time.[8] This method explores the slowly varying nature of the geomagnetic field. We can now solve the following Riccatti equation by eigenvector decomposition of an associated Hamiltonian matrix:

$$0 = -\boldsymbol{K}_\infty(t)\boldsymbol{W} - \boldsymbol{W}^T\boldsymbol{K}_\infty(t) - \boldsymbol{F} + \boldsymbol{K}_\infty(t)\boldsymbol{Q}(t)\boldsymbol{R}^{-1}\boldsymbol{Q}^T(t)\boldsymbol{K}_\infty(t) \tag{18}$$

and

$$0 = -\left[\boldsymbol{W}^T - \boldsymbol{K}_\infty(t)\boldsymbol{Q}(t)\boldsymbol{R}^{-1}\boldsymbol{Q}^T(t)\right]\boldsymbol{g}_\infty(t) + \boldsymbol{K}_\infty(t)\boldsymbol{N}_{\mathrm{con}} \tag{19}$$

This alternative method is computationally demanding because the Hamiltonian is a sixth-dimension matrix. But no large look-up tables are needed compared to the standard LQR method.

B. Minimum-Energy Controller

Another fixed terminating time, minimum-energy, optimal controller was presented[8] by minimizing the cost function subject to the constraint of Eq. (7) without the terms of N_T:

$$J = \frac{1}{2}\int_{t_0}^{t_f} \boldsymbol{M}^T\boldsymbol{M}\,\mathrm{d}t \tag{20}$$

The Hamiltonian function is as follows:

$$H = \tfrac{1}{2}\boldsymbol{M}^T\boldsymbol{M} + \boldsymbol{p}^T(t)[\boldsymbol{W}\boldsymbol{h} + \boldsymbol{Q}(t)\boldsymbol{M} + \boldsymbol{N}_{\mathrm{con}}] \tag{21}$$

The adjoint equations can be obtained as

$$\dot{\boldsymbol{p}}(t) = -\frac{\partial H}{\partial \boldsymbol{h}} = -\boldsymbol{W}^T\boldsymbol{p}(t) = \boldsymbol{W}\boldsymbol{p}(t) \tag{22}$$

The preceding equation is linear and can be solved analytically as

$$\boldsymbol{p}(t) = e^{Wt}\boldsymbol{p}(t_0) \tag{23}$$

The optimal control can then be obtained as

$$\boldsymbol{M}(t) = -\boldsymbol{Q}^T(t)\boldsymbol{p}(t) \tag{24}$$

and substituting Eq. (24) into Eq. (7) (without the term N_T), we obtain

$$\dot{\boldsymbol{h}}(t) = \boldsymbol{W}\boldsymbol{h}(t) - \boldsymbol{Q}(t)\boldsymbol{Q}^T(t)e^{Wt}\boldsymbol{p}(t_0) + \boldsymbol{N}_{\mathrm{con}} \tag{25}$$

The variation of extremals method[8,13] can now be used to solve for $\boldsymbol{p}(t_0)$ as follows:

1) Assume an initial $\boldsymbol{p}(t_0)$

2) Solve $\boldsymbol{h}(t)$ by numerically integrating Eq. (25) from t_0 to t_f, using $\boldsymbol{h}(t_0)$ and $\boldsymbol{p}(t_0)$ as initial conditions. Also, solve the state and costate influence function matrices $\boldsymbol{P}_h(t)$ and $\boldsymbol{P}_p(t)$ by numerical integration. We define

$$\boldsymbol{P}_h(t) \equiv \frac{\partial \boldsymbol{h}(t)}{\partial \boldsymbol{p}(t_0)}, \qquad \boldsymbol{P}_h(t_0) = [0] \text{ (the } 3\times 3 \text{ zero matrix)}$$

$$\boldsymbol{P}_p(t) \equiv \frac{\partial \boldsymbol{p}(t)}{\partial \boldsymbol{p}(t_0)}, \qquad \boldsymbol{P}_p(t_0) = [1] \text{ (the } 3\times 3 \text{ identity matrix)}$$

Using the relation of Eqs. (22–25), we take time derivative of $\boldsymbol{P}_h(t)$ and $\boldsymbol{P}_p(t)$, then

$$\dot{\boldsymbol{P}}_h(t) = \frac{\partial \dot{\boldsymbol{h}}(t)}{\partial \boldsymbol{p}(t_0)} = \boldsymbol{W}\boldsymbol{P}_h(t) + \boldsymbol{Q}(t)\boldsymbol{Q}(t)\boldsymbol{P}_p(t) \tag{26a}$$

$$\dot{\boldsymbol{P}}_p(t) = \frac{\partial \dot{\boldsymbol{p}}(t)}{\partial \boldsymbol{p}(t_0)} = \frac{\partial(\boldsymbol{W}\boldsymbol{p}(t))}{\partial \boldsymbol{p}(t_0)} = \boldsymbol{W}\boldsymbol{P}_p(t) \tag{26b}$$

3) Adjust $\boldsymbol{p}(t_0)$ based on Newton's method:

$$\boldsymbol{p}^{i+1}(t_0) = \boldsymbol{p}^i(t_0) - \left[\boldsymbol{P}_h^i(t_f)\right]^{-1}\boldsymbol{h}^i(t_f) \tag{27}$$

4) Repeat step 2 and 3 until $\|\boldsymbol{h}^i(t_f)\| < \varepsilon$, where ε is an arbitrarily small constant.

The MEC optimal control moment $\boldsymbol{M}(t)$ depends on the solution of $\boldsymbol{p}(t_0)$, and this can be done off-line for a specific orbit window. Note that the MEC controller will completely work in open loop as the solution for $\boldsymbol{M}(t)$ does not make use of any wheel momentum measurements.

Both LQR and MEC controllers just mentioned can be applied to achieve the optimal wheel momentum desaturation using three-axis magnetorquers. However, both these methods finally have to resort to solving the two-point boundary value problem[8,12] based upon the knowledge of the local geomagnetic field and require the amplitude of the moment of magnetic coils to be unbounded. The feedback nature of the LQR controllers would be preferred. The LQR controllers will ensure robustness against modeling errors and external disturbances. If the geomagnetic field does not change much between successive orbits, an orbital LQR gain look-up table can be calculated off line and then used onboard. The MEC controllers will consume the least amount of energy as expected. However, because of their open-loop nature and nonideal off-line calculations when solving the boundary-value problem, such as modeling errors (e.g., geomagnetic field) and external torque disturbances on the stabilized satellite, their control accuracy is limited.[8]

IV. Optimal Desaturation Controllers Using Pulse Width Modulated Thrusters

The thrusters could be employed to implement a relatively rapid management of the wheel momentum compared with magnetorquers. If the thrusters are used in the PWM mode, they can be approximated as linear actuators. The model of Eq. (7) in this case can be simplified as

$$\dot{\boldsymbol{h}}(t) = \boldsymbol{W}\boldsymbol{h}(t) + \boldsymbol{N}_T + \boldsymbol{N}_{\mathrm{con}} \tag{28}$$

A. Linear Quadratic Controllers

The optimal feedback control law to regulate the wheel momentum vector $\boldsymbol{h}$ toward the zero vector, using PWM thrusters, is derived by minimizing the following cost function:

$$J = \frac{1}{2}\int_{t_0}^{t_f} \left\{\boldsymbol{h}^T\boldsymbol{F}\boldsymbol{h} + \boldsymbol{N}_T^T\boldsymbol{R}\boldsymbol{N}_T\right\}\mathrm{d}t \tag{29}$$

To minimize the cost function in Eq. (29) subject to the desaturation model constraint of Eq. (28), we can solve the Riccatti equations (similar to that in Sec. III)

$$\dot{\boldsymbol{K}}(t) = -\boldsymbol{K}(t)\boldsymbol{W} - \boldsymbol{W}^T\boldsymbol{K}(t) - \boldsymbol{F} + \boldsymbol{K}(t)\boldsymbol{R}^{-1}\boldsymbol{K}(t) \tag{30}$$

and a vector differential equation

$$\dot{\boldsymbol{g}}(t) = -[\boldsymbol{W}^T - \boldsymbol{K}(t)\boldsymbol{R}^{-1}]\boldsymbol{g}(t) + \boldsymbol{K}(t)\boldsymbol{N}_{\mathrm{con}} \tag{31}$$

If we set weight matrixes $\boldsymbol{F}$ and $\boldsymbol{R}$ to be constant and diagonal, and make use of the boundary conditions $\boldsymbol{K}(t_f) = 0$ and $\boldsymbol{g}(t_f) = -\boldsymbol{R}\boldsymbol{N}_{\mathrm{con}}$, Eqs. (30) and (31) can easily be solved by backward integration methods. Therefore the control law is given by

$$\boldsymbol{N}_T(t) = -\boldsymbol{R}^{-1}\boldsymbol{K}(t)\boldsymbol{h}(t) + \boldsymbol{R}^{-1}\boldsymbol{g}(t) \tag{32}$$

The time-dependent 3×3 gain matrix $\boldsymbol{K}(t)$ and 3×1 vector $\boldsymbol{g}(t)$ can be saved in look-up tables to achieve onboard optimal desaturation control using PWM thrusters. If the infinite time LQR (ILQR) is adapted, the constant gain matrix $\boldsymbol{K}_\infty$ and vector $\boldsymbol{g}_\infty$ can be derived by

$$0 = -\boldsymbol{K}_\infty\boldsymbol{W} - \boldsymbol{W}^T\boldsymbol{K}_\infty - \boldsymbol{F} + \boldsymbol{K}_\infty\boldsymbol{R}^{-1}\boldsymbol{K}_\infty \tag{33}$$

$$0 = -\left[\boldsymbol{W}^T - \boldsymbol{K}_\infty\boldsymbol{R}^{-1}\right]\boldsymbol{g}_\infty + \boldsymbol{K}_\infty\boldsymbol{N}_{\mathrm{con}} \tag{34}$$

Because of the time invariance of the wheel momentum management model in Eq. (28), there is no need to build up the look-up gains in onboard memory or to solve the ILQR problem every sampling period. The gain matrix $\boldsymbol{K}_\infty$ and vector $\boldsymbol{g}_\infty$, because of the choice of the weighting matrixes $\boldsymbol{R}$ and $\boldsymbol{F}$, will determine the final response time of the desaturation system.

B. Minimum-Energy Controller

A fixed terminal time, minimum-energy optimal controller can be derived by minimizing the energy cost function subject to the constraint of Eq. (28):

$$J = \frac{1}{2}\int_{t_0}^{t_f} \boldsymbol{N}_T^T\boldsymbol{N}_T\,\mathrm{d}t \tag{35}$$

The optimal control torque will be

$$\boldsymbol{N}_T(t) = -\boldsymbol{p}(t) = -e^{Wt}\boldsymbol{p}(t_0) \tag{36}$$

and substituting Eq. (36) into Eq. (28) we obtain

$$\dot{\boldsymbol{h}}(t) = \boldsymbol{W}\boldsymbol{h}(t) - e^{Wt}\boldsymbol{p}(t_0) + \boldsymbol{N}_{\mathrm{con}} \tag{37}$$

The initial state $\boldsymbol{p}(t_0)$ of the costate vector $\boldsymbol{p}(t)$ in Eq. (37) can be solved off line as in Sec. III.

V. Combined Desaturation Controllers Using Magnetorquers and Thrusters

Magnetorquers and thrusters each have their own advantages and disadvantages for three-axis reaction-wheel momentum management. The advantages of magnetorquers are as follows: They do not generate translational forces, and therefore do not perturb the orbit; and they do not consume any thruster propellant. The disadvantage of magnetorquers is that the produced torque is relatively small, making the momentum dumping rate slow. The advantage of thrusters is that they can achieve rapid momentum dumping and remove much more momentum in a given period of time. The disadvantages of thrusters are as follows: They can consume expendable propellant, and they can generate translational forces to influence the satellite's orbit. Saving the thruster propellant is significant for an attitude control system equipped with thrusters. To date no published paper could be found that copes with the combined management of reaction-wheel momentum using magnetorquers and thrusters simultaneously. Next, we shall present an optimal combined control algorithm, and a combined control algorithm using a cross-product law, which makes full use of the advantages of magnetorquers and thrusters. The algorithms are simple and suitable for onboard real-time applications.

A. Optimal Combined Desaturation Controllers

The optimal LQR, ILQR, and MEC controllers for PWM control of thrusters just discussed can be used to obtain the dumping torque during a fixed time period from t_0 to t_f. If we want the torque $\boldsymbol{N}(k)$ at every sample time k to be generated simultaneously by magnetorquers and PWM thrusters, we can define

$$\boldsymbol{N}(k) = \boldsymbol{N}_T(k) + \boldsymbol{Q}(k)\boldsymbol{M}(k) \tag{38}$$

where $\boldsymbol{N}_T(k)$ is the three-axis PWM thruster torque and $\boldsymbol{Q}(k)$ is defined in Eq. (5). Equation (38) can be reorganized as

$$\boldsymbol{N}(k) = \boldsymbol{A}(k)\boldsymbol{N}_{\mathrm{MT}}(k) \tag{39}$$

where

$$\boldsymbol{A}(k) = \begin{bmatrix} 0 & B_z(k) & -B_y(k) & 1 & 0 & 0 \\ -B_z(k) & 0 & B_x(k) & 0 & 1 & 0 \\ B_y(k) & -B_x(k) & 0 & 0 & 0 & 1 \end{bmatrix}$$

$$\boldsymbol{N}_{\mathrm{MT}}(k) = [M_x(k) \quad M_y(k) \quad M_z(k) \quad N_{Tx}(k) \quad N_{Ty}(k) \quad N_{Tz}(k)]^T$$

To arrive at the formulation of an optimal combined controller, the following cost function is proposed:

$$J = \tfrac{1}{2}\boldsymbol{N}_{\mathrm{MT}}^T(k)\boldsymbol{S}\boldsymbol{N}_{\mathrm{MT}}(k) + \lambda^T[\boldsymbol{N}(k) - \boldsymbol{A}(k)\boldsymbol{N}_{\mathrm{MT}}(k)] \tag{40}$$

where λ is a 3×1 vector of Lagrange multipliers that adjoin the constant equations to the scalar cost equation and $\boldsymbol{S}$ is a 6×6 constant positive weighting matrix. We define $\boldsymbol{S}$ to be a diagonal positive matrix having the form

$$\boldsymbol{S} = \mathrm{diag}(a, a, a, b, b, b)$$

where a and b are positive scalars. To minimize J, we take derivatives of Eq. (40) with respect to $\boldsymbol{N}_{\mathrm{MT}}$ and λ giving the two vector equations:

$$\boldsymbol{N}(k) = \boldsymbol{A}(k)\boldsymbol{N}_{\mathrm{MT}}(k) \tag{41a}$$

$$\boldsymbol{N}_{\mathrm{MT}}(k) = \boldsymbol{S}^{-1}\boldsymbol{A}^T(k)\lambda \tag{41b}$$

Solving for $\boldsymbol{N}_{\mathrm{MT}}$, we obtain

$$\boldsymbol{N}_{\mathrm{MT}}(k) = \boldsymbol{S}^{-1}\boldsymbol{A}^T(k)[\boldsymbol{A}(k)\boldsymbol{S}^{-1}\boldsymbol{A}^T(k)]^{-1}\boldsymbol{N}(k) \tag{42}$$

Equation (42) is the optimal blending algorithm for magnetorquers and thrusters during wheel momentum management. This equation divides the required torque $\boldsymbol{N}(k)$ optimally into two parts. One part has to be generated by the magnetorquers and the other part by the PWM thrusters. The supporting torques produced by the magnetorquers could obviously reduce the consumption of the limited thruster propellant.

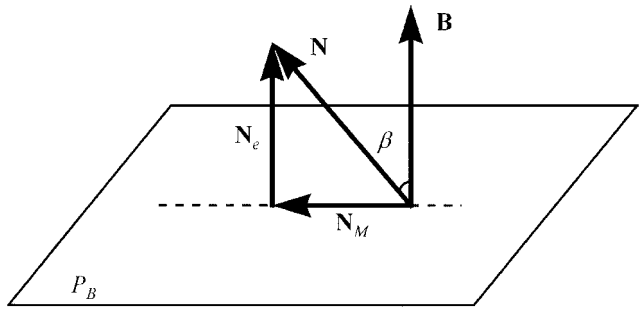

Fig. 1 Configuration of the favorable torque generated by magnetorquers.

B. Combined Desaturation Controllers Using a Cross-Product Law

The conventional well-known magnetorquing cross-product control[7,8] is given by

$$\boldsymbol{M} = -k_{\mathrm{cp}}(\boldsymbol{N} \times \boldsymbol{B})/\|\boldsymbol{B}\| \tag{43}$$

where $\boldsymbol{M}$ is regarded as the most favorable magnetorquing vector, $\boldsymbol{B}$ is the body geomagnetic field vector measured by onboard magnetometers, $\boldsymbol{N}$ is the required control torque vector, and k_{cp} is a constant scalar gain.

The active magnetic torque $\boldsymbol{N}_M$ must be in the plane P_B normal to the vector $\boldsymbol{B}$ shown in Fig. 1. We propose that the best torque $\boldsymbol{N}_M$ is one which is the projection of the desired $\boldsymbol{N}$ in plane P_B. This will be the minimum error condition. As a result, the desired $\boldsymbol{N}_M$ has the smallest error with respect to $\boldsymbol{N}$. The conventional cross product in Eq. (43) could not achieve this as it only ensures the correct vector direction for $\boldsymbol{N}_M$, but the magnitude of $\boldsymbol{N}_M$ will still depend on the scalar gain k_{cp}. Therefore, if we wish to minimize the error between $\boldsymbol{N}$ and $\boldsymbol{N}_M$, the cross-product law could be revised as

$$\boldsymbol{M} = -(\boldsymbol{N} \times \boldsymbol{B})/\|\boldsymbol{B}\|^2 \tag{44}$$

where the correct value for the scalar gain k_{cp} is inversely proportional to the magnetic field magnitude. According to the cross-product law in Eq. (44), the active magnetic torque vector $\boldsymbol{N}_M$ generated by magnetorquers is the projection of $\boldsymbol{N}$ in plane P_B in Fig. 1.

$$\boldsymbol{N}_M = \boldsymbol{M} \times \boldsymbol{B} = N \sin\beta \cdot (\hat{\boldsymbol{M}} \times \hat{\boldsymbol{B}}) \tag{45}$$

where N is the amplitude of the required torque vector $\boldsymbol{N}$, $\hat{\boldsymbol{M}}$ and $\hat{\boldsymbol{B}}$ are the unit vectors of $\boldsymbol{M}$ and $\boldsymbol{B}$, and β is the angle between the vectors $\boldsymbol{N}$ and $\boldsymbol{B}$.

Based upon the revised cross-product law for magnetorquer control, the combined controller for the management of RW momentum is derived by

$$\boldsymbol{N}(k) = \boldsymbol{N}_T(k) + \boldsymbol{N}_M(k) \tag{46}$$

where $\boldsymbol{N}_M(k)$ is the favorable torque by magnetorquers in Eq. (45). Therefore, $\boldsymbol{N}_T(k)$ must be equal to the torque error $\boldsymbol{N}_e$ in Fig. 1, which has the minimum amplitude. Additionally, the amplitudes of vectors $\boldsymbol{N}(k)$ and $\boldsymbol{N}_T(k)$ satisfy the following relation:

$$N(k) \geq N_T(k) \tag{47}$$

Equation (47) ensures that the PWM thrusters will minimize the fuel control energy during the combined management of the three-axis RW momentum.

VI. Comparison of the Desaturation Controllers

Simulations were implemented to investigate the performance of all of the RW momentum dumping controllers just analyzed. The satellite UoSAT-12 is used as an example during these simulations. The proposed methods will also be suitable for satellites in other operating conditions. UoSAT-12 is the first low-cost low-Earth-orbit (LEO) mini-satellite with three-axis Earth-pointing capability built by Surrey Space Center and equipped with three-axis reaction wheels, magnetorquers, and cold-gas thrusters. The satellite is expected to be launched in a 650-km circular orbit with an

inclination angle 65 deg during April of 1999. Its orbital period is nearly 100 min.

The Earth's magnetic field is simply defined as a first dipole model during simulations. In the local orbital coordinates the model for UoSAT-12 could be expressed as[8,10]

$$\boldsymbol{B}_o = \begin{bmatrix} B_{ox} \\ B_{oy} \\ B_{oz} \end{bmatrix} = \frac{M_e}{R_s^3} \begin{bmatrix} \sin i \cdot \cos\alpha \\ -\cos i \\ 2\sin i \cdot \sin\alpha \end{bmatrix} \tag{48}$$

where M_e is the vector geomagnetic strength of dipole, R_s is the geocentric position vector length, i is the inclination angle, and α is the orbit angle measured from the ascending node. During the simulations, we assumed that the cold-gas thrusters work in PWM mode with a minimum firing time of 50 ms each. The thruster torque has a constant value of ± 40 mNm during the active firing period. In addition, we assume the magnetic moment to be unbounded for the consideration of theoretical demonstration (The practical simulation for magnetic moment limit 40 Am^2 of UoSAT-12 will be discussed in the next section.). The sample time is 10 s. A perfect nadir-pointing attitude, i.e., $\boldsymbol{N}_{\text{con}} = 0$ in Eq. (7), is also assumed during simulations.

A. Simulations of Optimal Dumping Controllers Using Magnetorquers

The proposed optimal controllers LQR, ILQR, and MEC using magnetorquers only are compared with a conventional cross-product law (CCPL) dumping algorithm:

$$\boldsymbol{M} = K_m(\boldsymbol{h} \times \boldsymbol{B})/\|\boldsymbol{B}\| \tag{49}$$

where K_m is a scalar gain. To evaluate the performance of every controller, a control energy function for magnetic control moment $\boldsymbol{M}$ is defined as[4]

$$J_M(t) = \frac{1}{2}\int_{t_0}^{t} \boldsymbol{M}^T\boldsymbol{M}\,\mathrm{d}t \qquad t_0 \le t \le t_f \tag{50}$$

Figure 2 shows a half-orbit (3000-s) momentum dumping effort using the magnetorquer ILQR, LQR, MEC, and CCPL controllers (only the momentum amplitude $\|\boldsymbol{h}\|$ is shown). We can see the MEC controller consumes the least energy, and the energy cost of CCPL is the highest.

B. Simulation of Dumping Controllers Using Thrusters only and Combined Methods

Based upon the optimal controllers LQR, ILQR, and MEC using PWM cold-gas thrusters, the combined dumping algorithms were simulated and compared to the dumping controller using thrusters only (DCT). The energy function for the PWM cold-gas thrusters is also introduced as

$$J_{N_T}(t) = \frac{1}{2}\int_{t_0}^{t} \boldsymbol{N}_T^T\boldsymbol{N}_T\,\mathrm{d}t \qquad t_0 \le t \le t_f \tag{51}$$

Furthermore, the accumulated firing time of thrusters is investigated to assess the fuel consumption.

Figures 3 and 4 show a $\frac{1}{10}$-orbit (600-s) momentum dumping effort using thrusters only and the combined methods based upon the ILQR, LQR, and MEC controllers. Table 1 lists the overall results from the viewpoint of the propellant consumption and magnetorquer (MT) control energy cost for a $\frac{1}{10}$-orbit momentum dumping effort. The simulations show that the dumping performance of the controllers stays unchanged. When using thrusters only (DCT), the behavior of ILQR is almost the same as LQR. MEC consumes the least amount of control energy (shown in Fig. 4d), but its accumulated firing time is still almost the same as that of LQR. In addition, the combined dumping controllers based upon the revised cross-product law (CRCP) in Eq. (44) generally consumes the least amount of thruster propellant. The combined dumping controllers based upon the conventional cross-product law (CCCP) in Eq. (43) have the least thruster-fuel saving, and CCCP consumes the most magnetic control energy. The optimal combined desaturation controller (OCDC) in Eq. (42) tends to have the same effect as CRCP

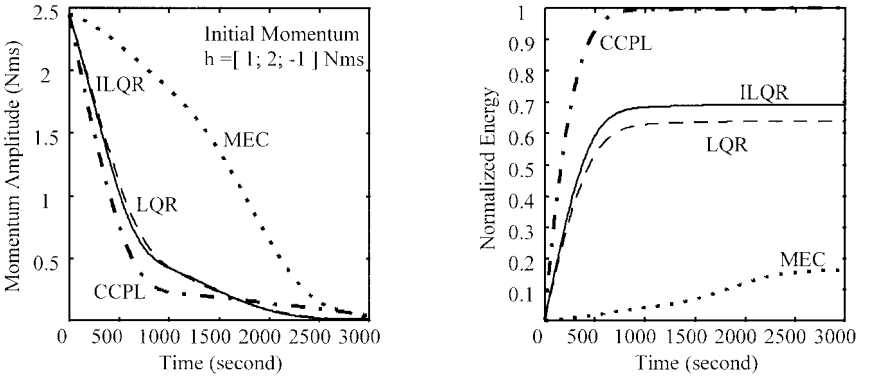

a) RW momentum b) Normalized magnetorquer control energy

Fig. 2 Momentum dumping using magnetorquers only.

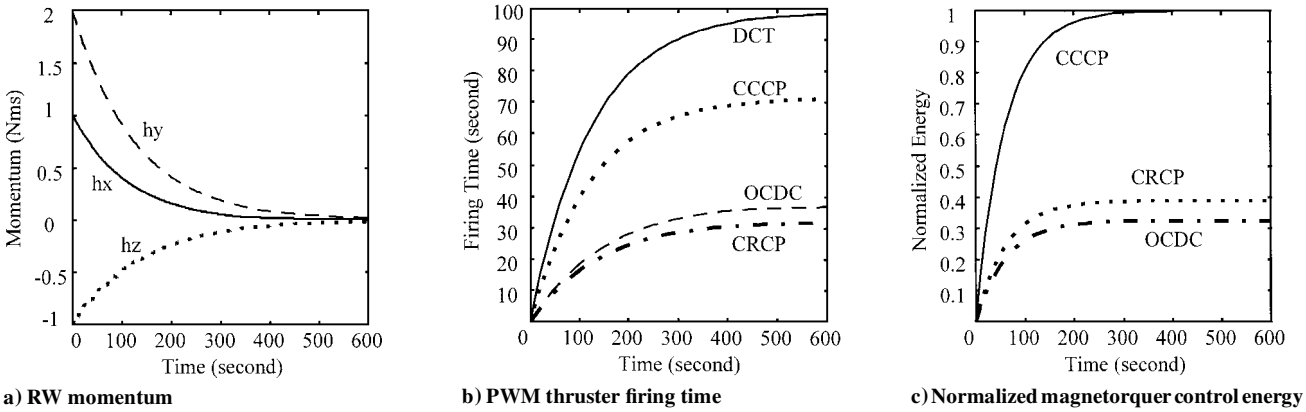

a) RW momentum b) PWM thruster firing time c) Normalized magnetorquer control energy

Fig. 3 Momentum dumping using thrusters only and combined methods based upon LQR.

Table 1 Comparison of the combined controllers

Dumping methods	ILQR, 0.1 orbit, 600 s			MEC, 0.1 orbit, 600 s		
Initial momentum, Nms	[1; 2; −1]	[2; −1.2; 0.5]	[1.2; −0.8; −2]	[1; 2; −1]	[2; −1.2; 0.5]	[1.2; −0.8; −2]
Starting point from ascending node, orbit	0.23	0.56	0.67	0.23	0.56	0.67
DCT						
CT firing time, s	98.25	87.75	95.30	93.90	88.15	89.35
CCCP						
CT firing time, sec	71.25	53.75	74.35	68.70	42.65	74.80
Fuel-saving, %	27.48	38.77	21.97	26.83	51.61	16.27
MT energy cost	1.00	1.00	1.00	1.00	1.00	1.00
CRCP						
CT firing time, s	31.95	52.80	56.00	39.50	31.35	50.75
Fuel-saving, %	67.48	39.83	41.23	57.93	64.43	43.21
MT energy cost	0.39	0.88	0.45	0.61	0.69	0.42
OCDC						
CT firing time, s	36.90	53.30	57.20	43.55	34.75	60.85
Fuel-saving, %	62.44	39.24	40.00	53.62	60.59	31.88
MT energy	0.33	0.63	0.37	0.21	0.50	0.35

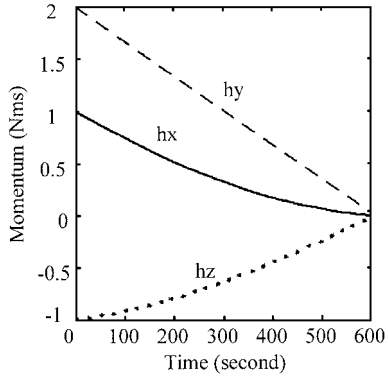

a) RW momentum

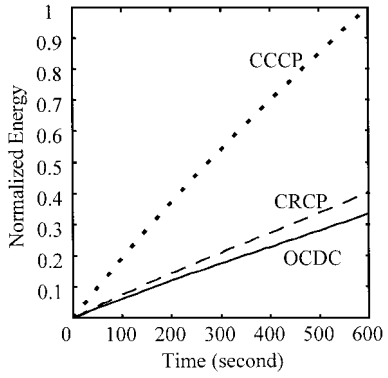

c) Normalized magnetorquer control energy

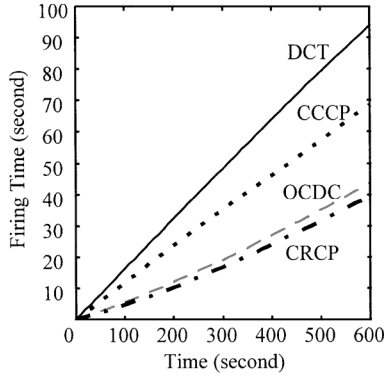

b) PWM thruster firing time

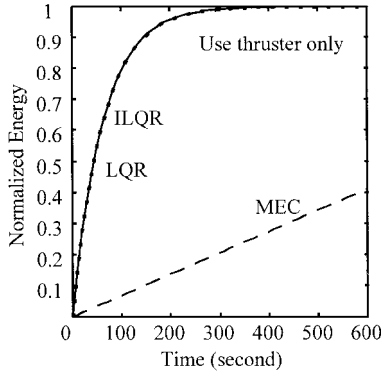

d) Normalized thruster control energy

Fig. 4 Momentum dumping using thrusters only and combined methods based upon MEC and DCT.

when the weighting matrix $\boldsymbol{S}$ has weight a as positively infinitesimal and weight b as positively infinite. This phenomenon can be explained by Fig. 1. For the OCDC in Eq. (42) to minimize the cost function in Eq. (40) requires that the weighting component a approaches zero and b approaches infinite. Then the thruster control vector $\boldsymbol{N}_T(k)$ will tend to be vector $\boldsymbol{N}_e$ in Fig. 1, which ensures the minimum-amplitude error between $\boldsymbol{N}$ and $\boldsymbol{N}_M$. Therefore, CRCP and OCDC could be the favored controllers for combined momentum dumping of magnetorquers and thrusters. In practice, CRCP will need less processing time. OCDC could balance the magnetic control energy cost and thruster fuel consumption by changing the weighting matrix $\boldsymbol{S}$.

VII. Discussion of Results

Combined RW momentum dumping algorithms were developed using an OCDC and a CRCP. The combined controllers rely only on the measured geomagnetic field $\boldsymbol{B}(k)$ and resort to a predetermined torque vector $\boldsymbol{N}(k)$, as calculated by the optimal LQR, ILQR, or MEC method in Sec. IV. However, the beneficial point is that the required control torque $\boldsymbol{N}(k)$ for dumping wheel momentum has been generated by an optimized blending of both magnetorquers and PWM cold-gas thrusters. This means that thruster propellant can be saved because of the assistance of the magnetorquers. Additionally, there is no need to predict off line the local geomagnetic field vector for these combined controllers. The magnetic field is simply obtained by magnetometer measurements. The control blending of the magnetorquers and thrusters can be computed easily from Eq. (42) or (46), making them useful for many practical applications.

As stated previously, all of these theoretical analyses assume that the magnetorquer control value is unbounded and continuous. In practice, the firing of magnetorquers cannot be allowed during the period of magnetometer measurements, and the magnetorquers also

Table 2 Momentum dumping using OCDC and thruster only (DCT) for UoSAT-12

Dumping methods	ILQR, 0.1 orbit, 600 s			MEC, 0.1 orbit, 600 s		
Initial momentum, Nms	[1; 2; −1]	[2; −1.2; 0.5]	[1.2; −0.8; −2]	[1; 2; −1]	[2; −1.2; 0.5]	[1.2; −0.8; −2]
Starting point from ascending node, orbit	0.23	0.56	0.67	0.23	0.56	0.67
DCT						
CT firing time, s	98.25	87.75	95.30	93.90	88.15	89.35
OCDC						
CT firing time, s	71.45	68.55	73.00	59.90	48.15	59.40
Fuel-saving, %	27.28	21.88	23.40	36.21	44.64	33.52

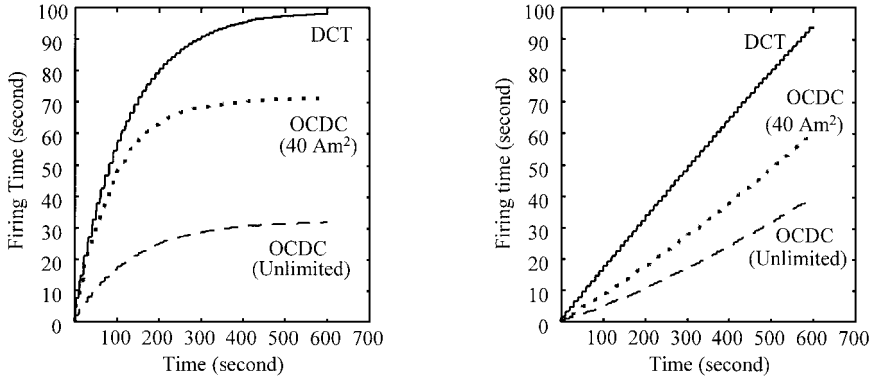

a) PWM thruster firing time of LQR **b) PWM thruster firing time of MEC**

Fig. 5 UoSAT-12 momentum dumping using thrusters only and combined method OCDC based upon ILQR and MEC.

have a saturation limit. This saturation limit may have a considerable effect. For UoSAT-12 the maximum magnetic dipole moment along every axis is nearly 40 Am^2. To model this saturation effect, we can add the following conditions to the simulation. If any component of $\boldsymbol{M}(k) = [M_x(k)\ M_y(k)\ M_z(k)]^T$ calculated from Eq. (42) or (46) exceeds the limit value, we can compensate the thruster control logic as follows:

$$\Delta \boldsymbol{N}_T(k) = \boldsymbol{Q}(k)[\boldsymbol{M}(k) - \boldsymbol{M}_{\max}] \tag{52}$$

where $\Delta \boldsymbol{N}_T(k)$ is the thruster compensated control vector and $\boldsymbol{M}_{\max}$ is the saturation value of magnetic moment. The thrusters also compensate for the lack of available magnetic torque.

The simulations of momentum management for the UoSAT-12 mission were repeated with the saturation constraint added. During the simulations, we assumed that magnetorquers also work in PWM mode with a minimum firing time of 50 ms each. The maximum firing time period is 9 s per sample time of 10 s. Figure 5 shows a comparison of thruster and magnetorquer activities for the combined method OCDC and for thruster only (DCT) during a $\frac{1}{10}$-orbit (600-s) RW momentum dumping effort. The momentum dumping behavior is the same as in Figs. 3 and 4. Table 2 lists several representative simulation results. Because of a variation of the geomagnetic field in orbit at different start positions during simulation, the thruster firing time will be different over similar dumping periods. However, the simulations show that the combined momentum dumping method can definitely save a large amount of thruster propellant.

VIII. Conclusions

RW momentum buildup because of secular disturbances can be reduced by actively applying compensating external torques of both three-axis magnetorquers and thrusters. The optimal LQR and MEC controllers discussed in this paper can be applied to achieve wheel momentum desaturation using three-axis magnetorquers and PWM thrusters separately. The LQR controllers are preferred because of their feedback nature. The MEC controllers will consume the least amount of energy. However, because of their open-loop nature and nonideal simulation conditions, such as modeling errors (e.g., geomagnetic field and the change of spacecraft inertia tensor caused by thruster propellant consumption) and external torque disturbances on the stabilized satellite, their control accuracy is limited. The optimal controllers using only magnetorquers strongly depend on the geomagnetic field model. If a detailed geomagnetic model is employed, a great computation effort is required to solve the two-point boundary problem for onboard applications.

The newly proposed combined dumping controllers exploit the merits of both magnetorquers and PWM thrusters. Based upon relatively simple thruster optimal algorithms, the blending methods effectively separate the required torques for magnetorquer and thruster commanding. They do not require geomagnetic field estimations but employ on-line magnetometer measurement data. Therefore, they could be suitable in practice for achieving rapid, propellant-saving three-axis RW momentum dumping. Simulation results demonstrate the merits of the proposed combined algorithms.

Acknowledgments

The authors wish to acknowledge the support given by Martin Sweeting and the Surrey Space Center ADCS team.

References

[1] Johnson, C. D., and Skelton, R. E, "Optimal Desaturation of Momentum Exchange Control Systems," *AIAA Journal*, Vol. 9, No. 1, 1971, pp. 12–22.

[2] Warren, W., Wie, B., and Geller, D., "Periodic-Disturbance Accommodating Control of the Space Station for Asymptotic Momentum Management," *Journal of Guidance, Control, and Dynamics*, Vol. 13, No. 6, 1990, pp. 984–992.

[3] Sunkel, J. W., and Shieh, L. S., "Optimal Momentum Management Controller for the Space Station," *Journal of Guidance, Control, and Dynamics*, Vol. 13, No. 4, 1990, pp. 659–668.

[4] Iida, H., and Keiken, N., "A New Approach to Magnetic Angular Momentum Management for Large Scientific Satellites," *NEC Research and Development*, Vol. 37, No. 1, 1996, pp. 60–77.

[5] Glaese, J. R., Kennel, H. F., Seltzer, S. M., and Sheldon, H. L., "Low-Cost Space Telescope Pointing Control System," *Journal of Spacecraft and Rockets*, Vol. 13, No. 7, 1976, pp. 400–405.

[6] Burns, T. F., and Flashner, H., "Adaptive Control Applied to Momentum Unloading Using the Low Earth Orbital Environment," *Journal of Guidance, Control, and Dynamics*, Vol. 15, No. 2, 1992, pp. 325–333.

[7]Chang, D. H., "Magnetic and Momentum Bias Attitude Control Design for the HETE Small Satellite," *Proceedings of the 6th AIAA/USU Conference on Small Satellites*, Utah State Univ., Logan, UT, 1992.

[8]Steyn, W. H., "Chapter 4: Momentum Dumping," *A Multi-Mode Attitude Determination and Control System for Small Satellites*, Ph.D. Dissertation, Dept. of Electronic Engineering, Univ. of Stellenbosch, South Africa, 1995, pp. 4-1–4-11.

[9]Martel, F., Pal, P. K., and Psiaki, M., "Active Magnetic Control System for Gravity Gradient Stabilised Spacecraft," *Proceedings of the Second AIAA/USU Conference on Small Satellites*, Utah State Univ., Logan, UT, 1988.

[10]Wertz, J. R., *Spacecraft Attitude Determination and Control*, D. Reidel Publishing Co., Dordrecht, The Netherlands, 1989, pp. 588–625.

[11]Larson, J. L., and Wertz, J. R., *Space Mission Analysis and Design*, Microcosm, Kluwer Academic, Norwell, MA, 1992, pp. 340–366.

[12]Burghes, D., and Graham, A., *Introduction to Control Theory Including Optimal Control*, Ellis Horwood, Chichester, England, UK, 1980, pp. 249–254.

[13]Kirk, D. E., *Optimal Control Theory, An Introduction*, Prentice–Hall, Englewood Cliffs, NJ, 1970, pp. 343–357.